Preprint – version 1
03.03.2023

Author:
Grigori Khvostov

Affiliation:
PSI – Switzerland

Title:
Calibration and Verification of thermal models of the FALCON code based on the first case of the first IAEA CRP FUMEX

Abstract:

Results of a model calibration-dedicated part of the project, entitled 'Comprehensive Verification of the FALCON Code for Calculation of Nuclear Fuel Temperature' are presented. For sensitivity analysis, Case 1 of the past IAEA CRP FUMEX is used. Considered are the effects caused by: correlations used for the fuel thermal conductivity; power maneuvering; fuel densification; treatment of the sinterable- and open- as-fabricated fuel porosity. After the calibration, essentially improved agreement with the data for FUMEX Case 1 is shown. A prerequisite for the following successful verification of the advanced version of the FALCON code as applied to fuel temperature during both SST- and transient- irradiation conditions is fulfilled through the current calibration.

Keywords:

FALCON code; GRSW-A model; Fuel temperature; Calibration; Verification; Fuel thermal conductivity; Fuel densification; Sinterable porosity; Open porosity

1. Introduction

Precise prediction of the fuel temperature in fuel rods of Light Water Reactors (LWRs) is one of the most important goals pursued by fuel behavior analysis codes. The calculated maximum fuel temperature itself is a limiting variable [1], which is directly related to a design criterion that requires avoiding of fuel melting during normal operation and Anticipated Operational Occurrences (AOOs). All the other safety and reliability criteria of fuel rods are strongly affected by the calculation of fuel temperature. Besides, prediction of the distribution of fuel temperature during base irradiation is necessary to define initial conditions for the analysis of Design Basis Accidents (DBAs), such as the Loss-Of-Coolant Accident (LOCA) and the Reactivity Initiated Accident (RIA).

In the last several years, special activities have been carried out within the STARS program at Paul Scherrer Institute (PSI) aiming at improved modeling of LWR fuel behavior in a wide range of irradiation conditions, including:

- Extension of the EPRI's FALCON code by coupling with the GRSW-A model [2] for fuel swelling and Fission Gas Release (FGR), resulting in creation and development of an advanced version of the code;
- Development of a FRELAX code and corresponding methodology [3-5] for the analysis of LOCA tests performed by the OECD Halden Reactor Project (HRP) [6];
- Development of a methodology for analysis of the HRP experiments on cladding 'lift-off' in LWR fuel rods [7];
- Development of a methodology for analysis of fuel behavior during an RIA [8,9];
- Development of special capability of code analysis restart [10], which allows for adequate simulation of fuel re-fabrication and modeling features of the thermo-couple sections in tested rods, etc.

The advanced version of the FALCON code was verified using the data for:

- FGR and Internal gas pressure in fuel rods;
- Fuel micro-structure, including distribution of the fission gases in fuel pellets and gaseous porosity;
- Fuel swelling due to gaseous pores and bubbles, and its effects on Pellet-Cladding Mechanical Interaction (PCMI).

Considerable improvement of the prediction capability of the advanced FALCON code was shown by the verification [10]. However, analysis revealed that the FALCON- predicted temperature of the fuel can significantly affect and be affected by predictions of the integrated GRSW-A model [11], whereas, by the beginning of the reporting activity, the code had not been verified against experimental data obtained from direct measurement of fuel temperature.

Therefore, a special research activity, entitled 'Comprehensive Verification of the FALCON Code for Calculation of Nuclear Fuel Temperature' was proposed and successfully implemented at Paul Scherrer Institute (PSI), within its STARS Program in the period 2020-22 [12,29]. This activity was focused on verification and improvement of predictions for the fuel temperature by the advanced FALCON code. Proper, high-quality data from the OECD/NEA International Fuel Performance Experiments (IFPE)

Database [13] was used, including datasets addressed by the past international code benchmark activities, viz.:

- FUMEX-I, carried out in the period from 1992 to 1996 [14];
- FUMEX-II, which took place in 2002-2006 [15];
- FUMEX-III, as conducted in 2008-2012 [16].

The general goal of the reporting project at PSI-STARS was achieved in a few steps. The current paper deals with the first step, which has been dedicated largely to calibration of the temperature-related models, which have been considered as uncertain. To this end, the data of Case 1 of the first IAEA Co-ordinated Research Programme (CRP) FUMEX was utilized, making the most of high quality of the corresponding dataset for the purpose of modeling, see Chapter 2, viz.: detailed specification of the tested rodlet and irradiation conditions, as was qualified through the use by many participants of FUMEX; availability of data for fuel temperature based on the on-line measurement; post-test analysis of the data pointing out to the trends in temperature, at fixed levels of Linear Heat Generation Rate (LHGR), with burnup; availability of data of Post-Irradiation Examination for Fission Gas Release (FGR) in the rodlet. Details of the proper analysis are presented in Chapter 3 through Chapter 5 of the current paper.

The FALCON code coupled to the GRSW-A models with the updated best-estimate modeling assumptions and parameters being 'frozen' was then employed in the further steps of verifications, namely:

- Fuel temperatures during the Steady-State (SST) irradiation in Cases 3.1/2/3 and Cases 4.A/B of FUMEX;
- Response of fuel temperature to a fast thermal transient using the data from two tests of the IFA-507 experimental series carried out by HRP;
- Integral thermal fuel behaviour during two power-bump tests of the RISOE-III project.

The results of the verification steps, just mentioned, are being published in the separate papers [17-19].

2. Experimental data

The main goal of the current step of the project was calibration of relevant models and analytical assumptions with expected uncertainty, or available alternatives that would result in the best selection to be further used throughout code verification, as well as its practical use in the future. To this end, the author has deliberately chosen one of the most straightforward, well-characterized (modeling-quality) cases, with the data being in the open public domain, i.e., Case 1 of the first IAEA CRP FUMEX [14], FU1.

The CRP FUMEX had a special focus on the thermal fuel behaviour. The cases, proposed for code benchmarking, incorporated data on fuel temperature, addressing low- and intermediate- levels of fuel burnup, viz.: fuel pellet fragment relocation, densification, pellet-cladding gap closure, effects of thermal conductivity degradation and feedback effects of fission gases on gap conductance, etc.

The main parameters of rod design and irradiation conditions for Case 1 of the FUMEX code benchmark are presented in Table 1.

Table 1: Parameters of fuel rod design and irradiation conditions for FUMEX Case 1 (FU1) [14]

Parameter (units)	Value
Rod Design	
Pellet radius, inner (mm)	0 (0.9 for thermocouple bore)
Pellet radius, outer (mm)	4.045
Pellet length (mm)	10
Pellet end geometry	Both ends dished, dish volume of 11 mm^3/pellet.
Cladding radius, inner (mm)	4.11
Cladding radius, outer, (mm	4.75
Active fuel stack length (mm	810
Total free volume (cm^3)	8.2
Filling gas	He
Filling gas pressure at RT (10^5 Pa)	10
Fuel surface roughness (μm)	2.0
Cladding surface roughness (μm)	0.5
Material Characteristics	
Enrichment by U235 (wt. %)	3.5
Fuel density (% of TD)	94.1
Open porosity (% of total porosity)	62
Increase in fuel density after re-sintering test, g/cm^3	0.1
Fuel grain size (μm)	10
Cladding type	Zry-4
Cladding yield stress at 400 °C (N/mm^2)	333
Irradiation conditions (HBWR)	
Fast flux level (n/cm^2-s)	$6.3\times10^{11}\times$LHGR(kW/m)
Coolant pressure (10^5 Pa)	33.6
Coolant temperature (°C)	240
Coolant/moderator	D_2O

All the experimental irradiations considered within FUMEX, including the current case, FU1, took place in the Halden Boiling Water Reactor (HBWR), under its natural conditions, viz.: advanced volumetric boiling of heavy water at a temperature of 240 ˚C and pressure of 3.4 MPa, and relatively low fast neutron flux. The data for FUMEX cases was provided, after proper processing by the Halden Rector Project (HRP), in the tabulated (i.e., provided in ASCII files) or graphical forms, including:

- LHGR as a function of time in nine equally-distanced axial nodes;
- LHGR in the upper thermocouple (TC) section of the fuel stack;
- HRP-supplied experimental estimates for evolution of centerline fuel temperature in the TC tip-node, at fixed values of LHGR, within a burnup range from 0 to 20 MWd/kgUO2;

- Fuel centerline temperature in the TC tip-node as a function of time, provided in the graphical form, which was tabulated for the current study by digitizing of the plot in Figure 5 of the IAEA Report [14];
- The data of Post -Irradiation Examination (PIE) for relative FGR at End-Of-Life (EOL) of the test.

3. Analytical tools and methods used for calculation

Calculations was performed using the FALCON code MOD01 Update31, as developed by ANATECH and EPRI [20,21]. The advanced version of the code, coupled with the GRSW-A model [11], version 4.03 [22] was employed.

Apart from model elements and parameters addressed by the calibration, see Chapter 4, standard models and approaches of FALCON were used for the calculations, viz.:

- Finite Element Method (FEM) based solution was employed for 2-dimentional thermo-mechanical state of the fuel stack and cladding.
- An axisymmetric rodlet was assumed and represented with the RZ- geometry.
- The SST operation-specific standard mesh was used for FEM analysis, viz.: 4 element columns, and 25 element rows in the fuel stack mesh; 3 element columns in cladding mesh.
- Default models of the FALCON code [20,21] were assumed in the analysis for elastic-visco-plastic deformation and creep in fuel and cladding, as well as fuel cracking and relocation, gap conductance, etc.
- Aspects of the code prediction relating to evolution of fuel microstructure, FGR, fuel swelling and densification have been analyzed by the integrated GRSW-A model [11].

Detailed axial distribution and history of LHGR were used as input for the FALCON code calculation, as shown in Figure 1. The analysis accounted for thermal and mechanical effects of the TC section in the fuel stack [7], see Figure 2, as well as the effect of hollow pellets in the upper part of the fuel stack on axial power distribution.

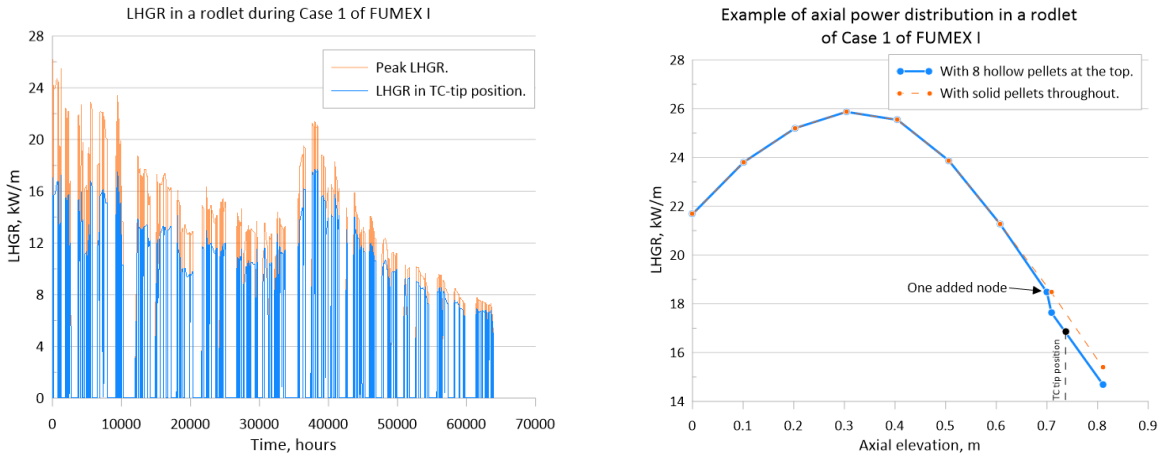

Figure 1: LHGR history (left) and axial power distribution (right) in the rod of FU1 case

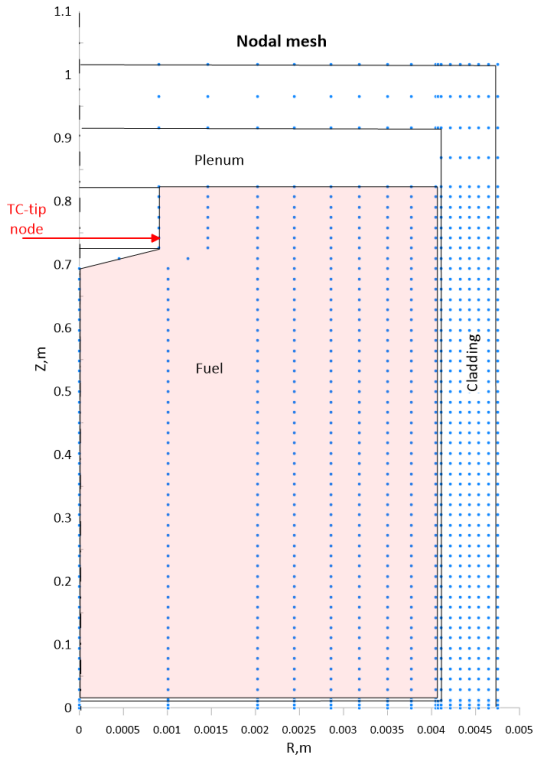

Figure 2: Rod nodal mesh with simulated TC section used for FU1 calculation

The FALCON's built-in enthalpy rise model [20,21] was employed for calculation of the cladding-coolant Heat Transfer Coefficients (HTC) and cladding outer surface temperature. Based on the calculation input for the coolant conditions, the Jens-Lottes correlation for HTC under fully developed boiling was automatically opted for, in agreement with the proper recommendation in Ref. [14].

4. Sensitivity-stipulated selection of modeling assumptions for calibration

As a system consisting of several interacting, relatively complex computational components, the FALCON code with the GRSW-A model needed finding out the best choice for a few correlations or assumed parameters of the models. Below discussed are the correlations and parameters that were shown to have considerable effect on predicted fuel temperature.

4.1. A Correlation for fuel thermal conductivity

A model for Fuel Thermal Conductivity (FTC) is expected to have significant effect on predicted fuel temperature. Generally, thermal conductivity of the solid UO2-based fuel is calculated as a sum of two terms, standing for heat conduction by the transport of phonons by the lattice, and electron conduction, λ_{ph} and λ_{el}, respectively:

$$\lambda_{th} = \lambda_{ph} + \lambda_{el} \qquad (1)$$

$$\lambda_{ph} = \frac{1}{A+BT} \quad (2)$$

$$\lambda_{el} = Ce^{DT} \quad (3)$$

where λ_{th} is the total thermal conductivity of the solid UO2 with the theoretical density assumed (pore-free), λ_{ph} the thermal conductivity due to phonon conduction by the lattice, λ_{el} the term representing electron conduction, *A* the model parameter describing the effect of phonon scattering by lattice impurities or discontinuities, *B* the model coefficient describing the effects of phonon-phonon collisions, *C* and *D* the constant parameters of the electron conduction term.

The lattice conduction term λ_{ph} dominates in the entire range of fuel temperature under the LWR operational conditions, while contribution of the electron heat conduction, λ_{el} becomes discernible at temperatures above ~1900 K. The lattice conduction-related part of thermal conductivity was shown to degrade with burnup due to buildup of the irradiation damage and fission product impurities within the UO2 matrix, which is simulated by treatment of the coefficients *A* and *B* as an increasing function of burnup. Additionally, experiments show that the degradation of thermal conductivity with burnup is subject to thermal recovery at a temperature above ~1100 K.

The calculation for UO2 FTC of the FALCON code has used, as a default model, the NFIR correlation [20], which treats the resulting lattice conductivity as a linear combination of the recovery-unaffected- and fully recovered- thermal conductivity components, viz.:

$$\lambda_{ph} = f_T \lambda_{end} + (1 - f_T)\lambda_{start} \quad (4)$$

where λ_{start} is the lattice conductivity before thermal recovery, λ_{end} the lattice conductivity after recovery, f_T the temperature-dependent coefficient of the model standing for fractional weight of the fuel with fully recovered thermal conductivity.

It is to be noted, that the NFIR model for FTC implies a relatively abrupt transition between no-recovery of the irradiation damage and the full recovery of irradiation damage, which is simulated with the thermal recovery function [20]:

$$f_T = 0.5\left[1 + tanh\left(\frac{T-1173}{150}\right)\right] \quad (5)$$

The details of the above-outlined NFIR correlation for FTC are presented in Ref. [20].

For the FALCON code with the integrated GRSW-A model, an alternative correlation [23] has been considered, as developed by Wiesenack and Nakamura [24,25], which is hereinafter referred to as W-N correlation. This assumes a conventional single-term treatment of the lattice conductivity (the first term in the right-hand side of Eq. 1):

$$\lambda_{th} = \frac{1}{0.0186T+5.16+f(b,T)} + 2.617\ 10^{-16}T^4 \quad (6)$$

where λ_{th} is the FTC (W/K-cm), *T* the temperature (K) in the range from 300 up to the melting point, *b* the burnup (MWd/kgU).

The function *f(b,T)* in Eq. 6 determines thermal conductivity degradation, in consideration of temperature-induced recovery:

$$f(b,T) = 100\,[\varphi(b) + h(T)g(b)] \qquad (7)$$

where $\varphi(b)=1.87\ 10^{-3}b$, $g(bu)=0.038b^{0.28}$, $h(T)=[1+198.\ exp(-6380/(T-273.))]^{-1}$.

As expected, calculation has shown considerable effect of the model for FTC on predicted fuel temperatures. For instance, Figure 3 shows distinct increase of the predicted peak centreline fuel temperature with transition to the W-N correlation in a rodlet of the FU1 case, assuming irradiation with constant power (left), and in a reference Case 27.2d of the CRP FUEMEX II [15] where a real PWR fuel rod is irradiated to a high burnup (right). As mentioned above, the calculated temperature has influenced other important variables of fuel state, specifically FGR. As shown in Figure 3 (right), higher values of FGR were predicted in the PWR rod throughout irradiation when the W-N correlation was used, which is more conservative, still being in a satisfactory agreement with the data for the ranges of measured FGR in sibling rods at different stages of irradiation, as shown by the blue vertical bars.

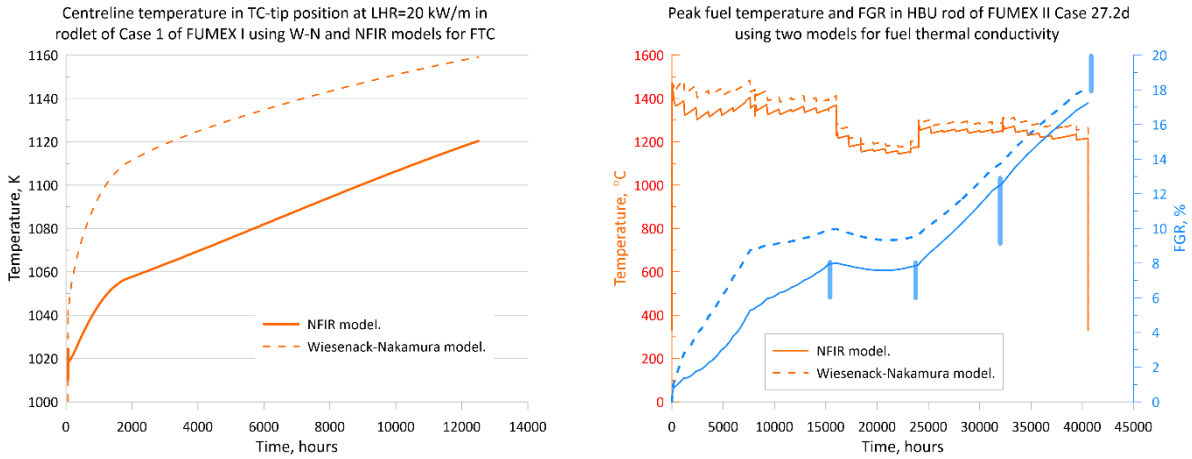

Figure 3: Effect of the model for fuel thermal conductivity on calculated fuel temperature

4.2. Effect of power maneuvering

As seen from Figure 4, for relatively low burnup, as, e.g., the one dealt with in the currently analyzed case, numerous variations of the rod power during irradiation (power maneuvering) were able to considerably affect the calculated pellet-cladding gap size and, consequently, pellet-cladding gap conductance, in comparison to irradiation with constant LHGR. As a result, the calculated fuel temperature in function of burnup, at the same fixed levels of LHGR, has turned out to be somewhat different for the calculations with constant power and variable (real) power history, see Figure 5.

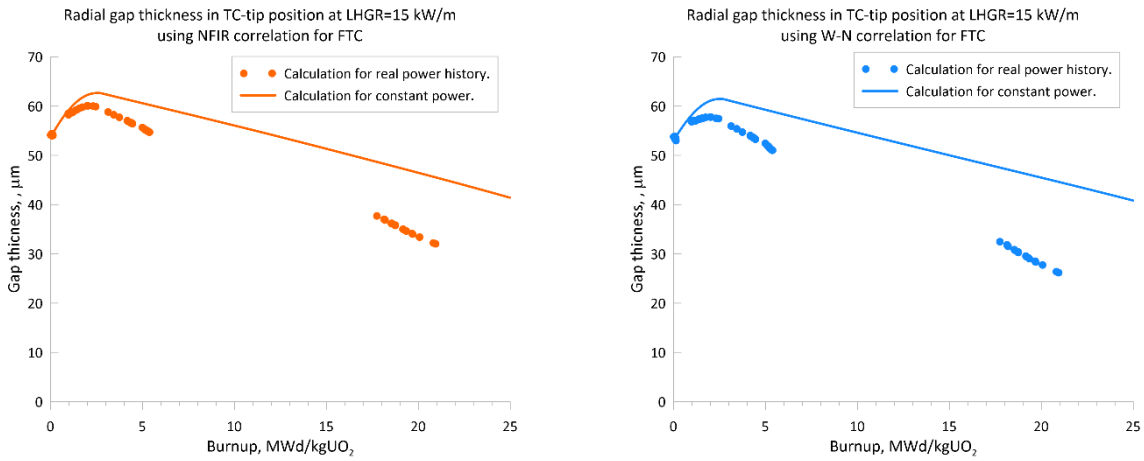

Figure 4: Calculated gap thickness at fixed power for the two FTC correlations

It is to be noted that in this and many other cases, the data was provided by the HRP to the IFPE Database and CRPs in the form of temperature as a function of local pellet-averaged burnup at fixed values of LHGR. These considerations have, eventually, motivated including the effect of power maneuvering into the generalized sensitivity analysis of the current FALCON modeling optimization for fuel temperature calculations.

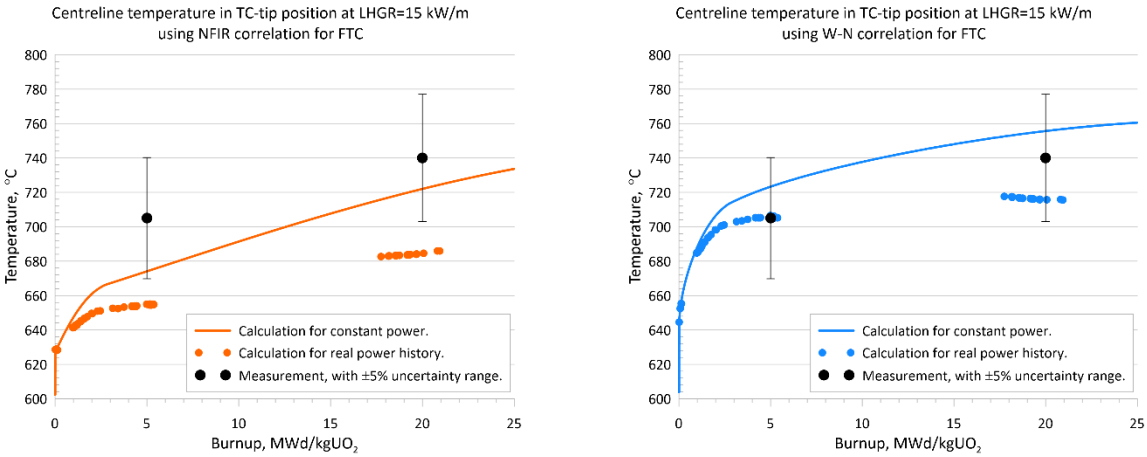

Figure 5: Calculated fuel temperature at fixed power assuming the real (maneuvering-) and constant-power history

4.3. Treatment of sinterable porosity in FALCON–to–GRSW-A coupling schema for thermal calculation

Eq. 1 and Eq. 6 are written for thermal conductivity of UO2 fuel with the theoretical density. To account for the decrease in FTC due to fuel porosity, a porosity-dependant multiplier has been introduced [26,27], viz.:

$$\lambda = \lambda_{th} \times (1 - P)^{2.5} \qquad (8)$$

where λ is the resulting thermal conductivity, λ_{th} thermal conductivity of fuel with the theoretical density, P the total fuel porosity (unitless).

Calculation of the total fuel porosity, P accounts for contribution of the as-fabricated pores, P_0, and the gaseous pores formed during the irradiation, P_G:

$$P = P_0 + P_G \tag{9}$$

Calculation of the gaseous porosity is provided by the complex analysis of the GRSW-A model [11]. The initial value of as-fabricated porosity is directly linked with the initial fuel density, according to the fuel specification:

$$P_0 = 1 - \frac{\rho_0}{\rho_{TD}} \tag{10}$$

where ρ_0 is the initial density, ρ_{TD} the theoretical density.

On the other hand, the as-fabricated porosity is treated as variable too, because a certain part of this is vanished in the beginning of irradiation due to irradiation-induced densification, or high-temperature sintering of the fine, uniformly distributed pores [28], which is also simulated by the GRSW-A model.

As far as the effect of sinterable porosity on calculated FTC is concerned, the coupling schema of the FALCON code and GRSW-A model has implied the use of one of the two options, to be selected by the user through an input parameter, IFGFTHC [22], hereinafter referred to as the T-coupling parameter, viz.:

- IFGFTHC=1, when a model for FTC uses porosity as calculated by GRSW-A, including evolution of the sinterable as-fabricated porosity. Individual degradation-term is imposed on every integration point of the fuel mesh, or
- IFGFTHC=2, which is like IFGFTHC=1, but without the effect of vanishing of the sinterable porosity in the calculation of thermal conductivity.

As shown in Figure 6, the assumed T-coupling parameter can considerably affect the calculated fuel temperature, especially in the beginning of irradiation. Consequently, the coupling schema between the FALCON code and GRSW-A for the effect of sinterable as-fabricated porosity on FTC has been included in the current calibration.

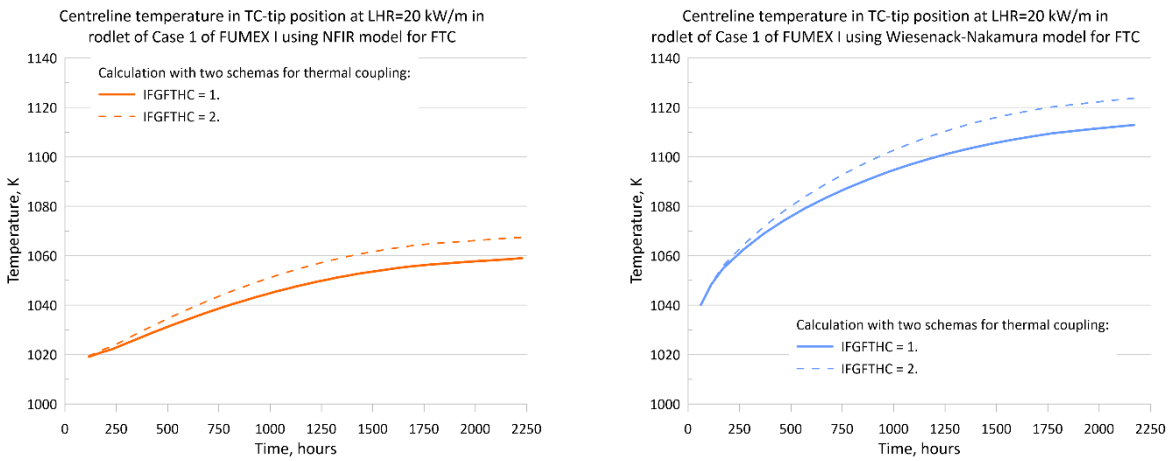

Figure 6: Effect of the FALCON–to–GRSW-A thermal coupling schema on fuel temperature

4.4. Effect of fuel densification

Another modelled consequence of the presence of sinerable porosity in the fuel is a decrease in pellet volume due to the pore vanishing resulting from irradiation-induced densification or high-temperature sintering [11]. Pellet densification causes an increase in the pellet-cladding gap size and, therefore, affects fuel temperature, as shown in Figure 7.

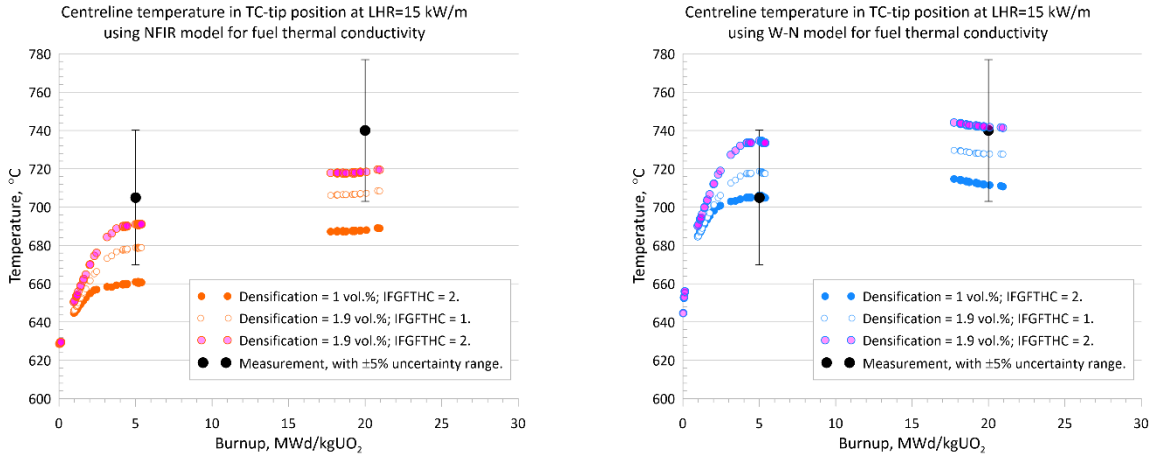

Figure 7: Effect of pellet densification on calculated fuel temperature

The value of sinterable porosity to be used by the GRSW-A model for calculation of fuel densification is defined from the FALCON's input parameter RHOOUT [21] specifying the increase in fuel density after densification:

$$P_s = \frac{\Delta\rho_s}{\rho_{TD}} \qquad (11)$$

where P_s is the volumetric sinterable porosity (unitless), $\Delta\rho_s$ the increase in fuel density after a re-sintering test, ρ_{TD} the theoretical density (10.98 g/cm^3).

Substitution of the specified value for the increase in fuel density after a re-sintering test (Table 1) in Eq. 11 yields a sinterable porosity of 1 vol.% in the FU1 case.

On the other hand, Ref. [14] recommends using a value of siterable porosity to be obtained from calculation tuning, to fit a temperature increase of 60°C due to pellet densification after irradiation with LHGR=20 kW/m over burnup range from 0 to 3.5 MWd/kgUO2. This approach resulted in estimated sinterable porosity of 1.9 vol.%, when using the NFIR correlation for FTC.

4.5. Correlation between volumetric open porosity and specific open surface area

As the fuel of the FU1 case had an extraordinarily high fraction of open pores (i.e., 62 % of the total as-fabricated porosity is due to open pores, see Table 1), calculation had to be performed using a proper correlation between the volumetric open porosity and the specific surface area of the open pores.

In this respect, the input system of the integrated GRSW-A code handles two options, depending on a special input parameter, IFGFTHC_FOP:

$$\begin{cases} \left(\frac{S}{V}\right)_{open} = 3.25\ {P_0}^{2.8}, & if\ IFGFTHC_{FOP} = 02 \\ \left(\frac{S}{V}\right)_{open} = 3.25\ {P_0}^{2.8} \times \left(\frac{P_{open}}{0.5}\right)^{0.65}, & if\ IFGFTHC_{FOP} = 12 \end{cases} \quad (12)$$

where P_{open} is the volumetric open porosity (vol.%), $(S/V)_{open}$ the specific surface area of the open pores.

A special multiplier, f_{op} was introduced into the correlation Eq. 12 to account for dependency of the specific open surface area in the fuel on a fraction of open pores in the total as-fabricated porosity, upon IFGFTHC_FOP = 12:

$$\left(\frac{S}{V}\right)_{open} = 3.25\ {P_0}^{2.8} \times \left(\frac{f_{op}P_0}{0.5}\right)^{0.65} \quad (13)$$

where f_{op} is the fractional open volumetric porosity, as introduced through a FALCON's input file, the command card '*FUEL' [21]; The second multiplier on the right-hand side of the above equation takes account of deviations from the standard value of open porosity, typically amounting to ~10 % of the initial total porosity in LWR fuels with a density of ~95 % TD.

After this modification, the calculation for FGR in the rodlet of the FU1 case has shown good agreement with the data for EOL FGR as measured by rod puncturing, see Figure 8.

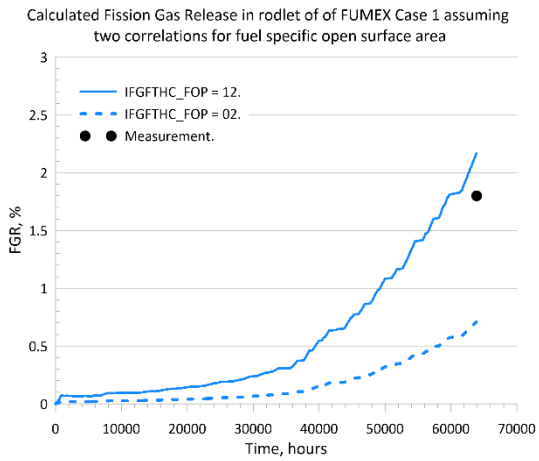

Figure 8: Effect of a correlation used for specific open surface area in the fuel on calculated FGR

5. Results and discussion

The calibration was carried out with a view to finding the best modeling assumptions, to fit the following experimental data:

- Temperature increases at LHGR=20 kW/m over burnup range from 0 to 3.5 MWd/kgUO2. Although assessment of this value in the TC-node of the rodlet was not possible when using the real power history, as the local LHGR in the TC-node had never reached a level of 20 kW/m, a value of 60°C was recommended in the IAEA report [21] as a generalized experimental observation. Consequently, the corresponding calculation was performed assuming a hypothesized irradiation with a constant power of 20 kW/m.
- Temperature at LHGR =15 kW/m and a burnup of 5 MWd/kgUO2.
- Temperature at LHGR =15 kW/m and a burnup of 20 MWd/kgUO2.
- Temperature increases at LHGR = 15 kW/m over a range of burnup from 5 to 20 MWd/kgUO2.

The last three values were calculated using the real power history in the rodlet during irradiation in the Halden reactor, as well as assuming a hypothesized irradiation with a constant power of 15 kW/m.

Based on the discussion of Chapter 4, the original and alternative assumptions were investigated for the following:

- *A model for FTC:* The original NFIR model, as supplied to the FALCON code, was assumed as the base case. An alternative (W-N) correlation was implemented and considered by the sensitivity analysis.
- *A parameter IFGFTHC of FALCON –to–GRSW-A thermal coupling (T-coupling parameter):* The base assumption, with IFGFTHC=1, suggested that calculation of FTC used a value of as-fabricated porosity as calculated by GRSW-A, including vanishing of the sinterable as-fabricated porosity. An alternative approach, upon IFGFTHC=2, excluded the effect of sinterable (vanishing) as-fabricated porosity due to densification on the calculated FTC.
- *A value of volumetric fuel densification during the low-burnup phase of irradiation:* The base case for this parameter, amounting to 1.0 vol%, was selected based on the available data for increase in fuel density after a re-sintering test. An alternative value of 1.9 vol.% was obtained

by tuning of the calculation with the base (NFIR) model for FTC, to fit the recommended value of 60°C for temperature increase at LHGR=20 kW/m over a burnup range from 0 to 3.5 MWd/kgUO2.

- *A type of power history assumed in the calculation:* The real power history in the rodlet of the FU1 case was assumed as the base case. Because the results obtained have shown complex sensitivity to power maneuvering, alternative calculation for the hypothesized irradiation, with constant power, was carried out.

The results of calculation versus the data, using different combinations of the above-listed base- and alternative- modeling assumptions are put together in Table 2 through Table 5. Note that the current results were obtained by setting none, one, or two of modeling assumptions to their alternative variant, at the others being set to the base ones.

Table 2: Temperature increase at LHGR = 20 kW/m over burnup range from 0 to 3.5 MWd/kgUO2 (°C)

		FTC model		T-coupling parameter		Densification, vol.%		LHGR history	
		NFIR	W-N	1	2	1.0	1.9	Real	Const.
FTC correlation	NFIR	**41**		41	48	41	68	-	41
	W-N		**73**	73	84	73	96	-	73
T-coupling parameter	1	41	73	**41**		41	68	-	41
	2	48	84		**48**	48	85	-	48
Densification, vol.%	1.0	41	73	41	48	**41**		-	41
	1.9	68	96	68	85		**68**	-	68
LHGR history	Real	-	-	-	-	-	-	-	
	Const.	41	73	41	48	41	68		**41**
Experimental estimate, °C		**≈ 60**							

Table 3: Temperature at LHGR=15 kW/m and a burnup of 5 MWd/kgUO2 (°C)

		FTC model		T-coupling parameter		Densification, vol.%		LHGR history	
		NFIR	W-N	1	2	1.0	1.9	Real	Const.
FTC correlation	NFIR	**655**		655	661	655	679	655	668
	W-N		**699**	699	706	699	719	699	715
T-coupling parameter	1	655	699	**655**		655	679	655	668
	2	661	706		**661**	661	691	661	674
Densification, vol.%	1.0	655	699	655	661	**655**		661	668
	1.9	679	719	679	691		**679**	679	691
LHGR history	Real	655	699	655	661	655	679	**655**	
	Const.	668	715	668	674	668	691		**668**
Measurement, °C		**704 ± 35**							

Table 4: Temperature at LHGR=15 kW/m and a burnup of 20 MWd/kgUO2 (°C)

		FTC model		T-coupling parameter		Densification, vol.%		LHGR history	
		NFIR	W-N	1	2	1.0	1.9	Real	Const.
FTC correlation	NFIR	**685**		685	688	685	707	685	717
	W-N		**707**	707	712	707	728	707	750
T-coupling parameter	1	685	707	**685**		685	707	685	717
	2	688	712		**688**	688	718	688	722
Densification, vol.%	1.0	685	707	685	688	**685**		685	717
	1.9	707	728	707	718		**707**	707	740
LHGR history	Real	685	707	685	688	685	707	**685**	
	Const.	717	750	717	722	717	740		**717**
Measurement, °C		**740 ± 37**							

Table 5: Temperature increase at LHGR=15 kW/m over a range of burnup from 5 to 20 MWd/kgUO2 (°C)

		FTC model		T-coupling parameter		Densification, vol.%		LHGR history	
		NFIR	W-N	1	2	1.0	1.9	Real	Const.
FTC correlation	NFIR	**30**		30	27	30	28	30	49
	W-N		**8**	8	6	8	9	8	35
T-coupling parameter	1	30	8	**30**		30	28	30	49
	2	27	6		**27**	27	27	27	48
Densification, vol.%	1.0	30	8	30	27	**30**		24	49
	1.9	28	9	28	27		**28**	28	49
LHGR history	Real	30	8	30	27	30	28	**30**	
	Const.	49	35	49	48	49	49		**49**
Measurement, °C		**≈ 35**							

Analysis of the sensitivity matrix in question against the proper experimental data has resulted in suggested modifications in the best assumptions to be used for calculation of fuel temperature with the FALCON code coupled to the GRSW-A, as presented in Table 6. Note that the calibration, as presented in Table 6, has included, also, the model for specific surface area of open pores, as discussed in sub-chapter 4.5, noting that the results of calculation shown in Figure 8 were obtained with all the other modeling assumptions corresponded to their variants after the calibrations.

Table 6: Best-estimate assumptions for selected models and parameters before and after calibration

Model/Parameter	**Best assumption**	
	Before calibration	**After calibration**
A model for FTC	NFIR	W-N
T-coupling parameter (IFGFTHC)	With effect of fuel densification on FTC (IFGFTHC =1)	Without effect of fuel densification on FTC (IFGFTHC =2)
Volumetric fuel densification, vol.%	Based on the data from high-temperature re-sintering test (1.0 vol.%)	
Assumed type of power history	Real	Const. or real
Specific surface area of open pores (IFGFTHC_FOP)	Open pore fraction-independent (IFGFTHC_FOP=02)	Open pore fraction-dependent (IFGFTHC_FOP=12)

Summarizing the results of the current sensitivity analysis together, the following conclusions can be proposed:

- The new (W-N) correlation for FTC seems to be preferable, in comparison to the original (NFIR) one, for calculation of fuel temperature with FALCON coupled to the GRSW-A model.
- After the current calibration, the re-sintering data-based value for fuel densification can be used, as-is.
- A reduced T-coupling schema (IFGFTHC=2) seems to be preferable, in consideration of the calculation conservatism, noting that for the real modern fuels the influence of this parameter is essentially reduced due to optimization of the fuel dimensional stability by reduction of the sinterable as-fabricated porosity.
- Finally, after model calibration, simulations with both real (maneuvering) and idealized (constant) power histories yielded results falling in the corresponding measurement uncertainty bands. Both types of calculations seem to be satisfactory in comparison to the measurement, and can be employed, noting that the results obtained with the constant power compares somewhat better with this experimental data.

The calculated fuel centreline temperature in the TC-tip position of the rodlet during irradiation of the FUMEX Case 1 is shown in Figure 9 against the data of on-line measurement. The calculation vs. measurement for temperature at a fixed LHGR of 15 kW/m is shown in Figure 10. The calibrated code has predicted temperatures within 5% tolerance band of the measurement up to a burn-up of ca. 20 MWd/kgUO2, while the original calculation systematically underpredicted temperature.

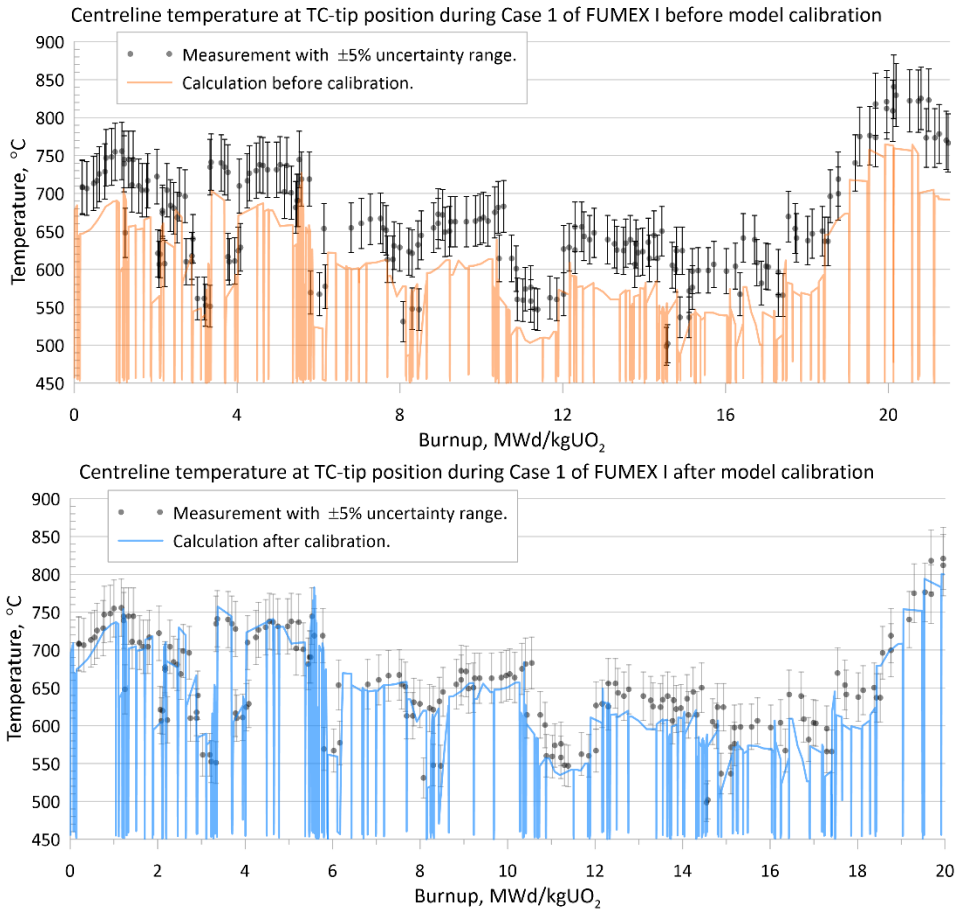

Figure 9: Calculated vs. measured temperature during irradiation before (top) and after (bottom) calibration.

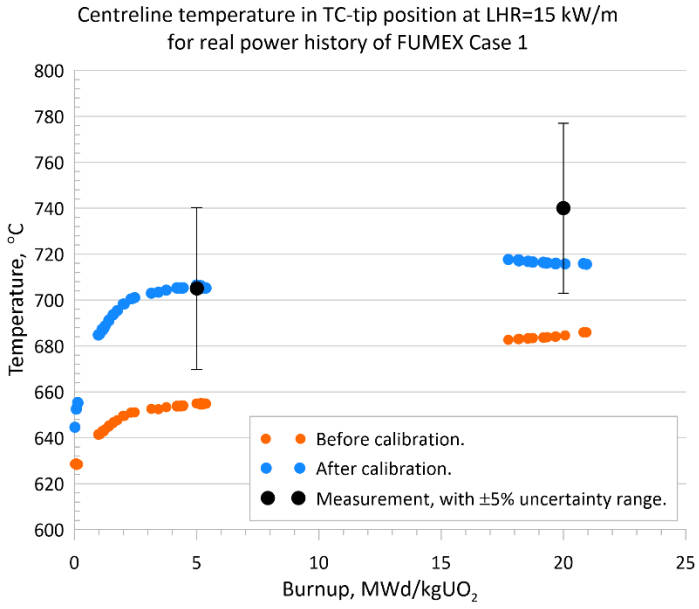

Figure 10: Calculation vs. measurement for temperature at a fixed LHGR of 15 kW/m before (top) and after (bottom) calibration

The FALCON code with the GRSW-A model using the updated best-estimate assumptions, as discussed in the current chapter, has been used in all the calculations of the reporting project, addressing fuel temperature during both SST- and transient- irradiation conditions. Outcomes of this verification are being published in separate papers [17-19], noting that in all the cases considered the calculation has shown good agreement with experimental data, like in the current FUMEX Case1.

6. Conclusions

A research project entitled 'Comprehensive Verification of the FALCON Code for Calculation of Nuclear Fuel Temperature' was proposed and successfully implemented at Paul Scherrer Institute (PSI) under the auspice of the STARS/ENSI RND Programme 2020-22. The research activity pursued the goal of proper verification of the advanced version of the code for calculation of fuel temperature, in consideration of modifications made in the standard FALCON code.

The current article presents the results of the part of the project dedicated to calibration of uncertain elements of modeling, based on sensitivity analysis against the data of a reference irradiation test conducted in the Halden Boiling Water Reactor (HBWR). Specifically, Case 1 of the past IAEA CRP FUMEX was used, thanks to relatively high quality of the corresponding dataset from the viewpoint of modeling.

The analysis addressed effects on calculated temperature, cause by: A correlation used for the fuel thermal conductivity; Power maneuvering; Fuel densification; Treatment of the sinterable- and open-as-fabricated fuel porosity. After the calibration, the calculation has shown essentially improved agreement with the data for FUMEX Case 1. The FALCON code with the GRSW-A model using the updated best-estimate assumptions was further used in all the calculations of the reporting project, addressing fuel temperature during both SST- and transient- irradiation conditions. Outcomes of this verification are being published in separate papers, noting, that in all the cases considered, the calculation has shown good agreement with experimental data, like in the current FUMEX Case1.

Acknowledgement

The reporting research activity was carried out at Paul Scherrer Institute (PSI – Switzerland) within the STARS/ENSI RND Programme 2020-22, which was supported by the Swiss Nuclear Safety Inspectorate (ENSI). The author is deeply grateful to Dr. Gorzel, Andreas (ENSI) for his continuous interest in, and fruitful collaboration on nuclear safety-related aspects of LWR fuel behavior modeling.

References

1. Nuclear Fuel Safety Criteria Technical Review (second edition), ISBN 978-92-64-99178-1, OECD 2012.
2. G. Khvostov, "A Dynamic Model for Fission Gas Release and Gaseous Swelling Integrated into the FALCON Fuel Analysis and Licensing Code", Proc. TOP Fuel 2009, Paris, France, September 6-10, 2009, Paper 2085.
3. G. Khvostov, A. Romano, M.A. Zimmermann, "Modeling the effects of axial fuel relocation in the IFA-650.4 LOCA test", Enlarged Halden Programme Group Meeting 2007, Storefjell Hotel, Gol, Norway, 11–16 March, 2007, Paper F4.7.
4. G. Khvostov, W. Wiesenack, M. A. Zimmermann, and G. Ledergerber, "Some insights into the role of axial gas flow in fuel rod behaviour during the LOCA based on Halden tests and calculations with the FALCON-PSI code", Nucl. Eng. Des., vol. 241, no. 5, pp. 1500-1507, 2011. https://doi.org/10.1016/j.nucengdes.2011.03.003.
5. G. Khvostov, "Modelling effects of transient FGR in LWR fuel rods during a LOCA", J. Nucl. Mater., vol. 559, p. 153446 (26 pp.), 2022. https://doi.org/10.1016/j.jnucmat.2021.153446.
6. W. Wiesenack. Summary of the Halden Reactor Project LOCA Test Series IFA-650. OECD HRP, 2013.
7. G. Khvostov and W. Wiesenack, "Analysis of selected Halden overpressure tests using the FALCON code", Nucl. Eng. Des., vol. 310, pp. 395-409, 2016. https://doi.org/10.1016/j.nucengdes.2016.10.033.
8. G. Khvostov, "Models for numerical simulation of burst FGR in fuel rods under the conditions of RIA", Nucl. Eng. Des., vol. 328, pp. 36-57, 2018. https://doi.org/10.1016/j.nucengdes.2017.12.028.
9. G. Khvostov and A. Gorzel, "FALCON code-based analysis of PWR fuel rod behaviour during RIA transients versus new U.S.NRC and current Swiss failure limits", Nucl. Eng. Technol., vol. 53, no. 11, pp. 3741-3758, 2021. https://doi.org/10.1016/j.net.2021.06.001.
10. F. Ribeiro and G. Khvostov, "Multi-scale approach to advanced fuel modelling for enhanced safety", Prog. Nucl. Energy, vol. 84, pp. 24-35, 2015. https://doi.org/10.1016/j.pnucene.2015.03.022.
11. G. Khvostov, K. Mikityuk, and M. A. Zimmermann, "A model for fission gas release and gaseous swelling of the uranium dioxide fuel coupled with the FALCON code", Nucl. Eng. Des., vol. 241, no. 8, pp. 2983-3007, 2011. https://doi.org/10.1016/j.nucengdes.2011.06.020.
12. H. Ferroukhi. Proposal STARS/ENSI RND Activities 2020-2022. SB-PL-REC-010-19, PSI, September 2019.
13. OECD/NEA International Fuel Performance Experiments (IFPE) Database. Web.: https://www.oecd-nea.org/jcms/pl_36360/ifpe-content.
14. Fuel modelling at extended burnup. Report of the Co-ordinated Research Programme on Fuel Modelling at Extended Burnup — FUMEX 1993-1996. IAEA-TECDOC-998.
15. Fuel Modelling at Extended Burnup (FUMEX-II). Report of a Coordinated Research Project 2002–2007. IAEA-TECDOC-1687.

16. Improvement of Computer Codes Used for Fuel Behaviour Simulation (FUMEX–III). REPORT OF A COORDINATED RESEARCH PROJECT 2008–2012. IAEA-TECDOC-1697.
17. G. Khvostov, “Analysis of thermal fuel behaviour under steady-state irradiation using the FALCON code as applied to selected cases of CRP FUMEX ”, manuscript draft, 2023.
18. G. Khvostov, “Insights into transient thermal fuel beahaviour based on calculation for two tests of the IFA-507 experiment using the FALCON code”, manuscript draft, 2023.
19. G. Khvostov, “Interpretation of the online measurement data on thermal fuel behavior during the two bump-tests of the RISOE-III project”, manuscript draft, 2023.
20. Fuel Analysis and Licensing Code: FALCON MOD01: Volume 1: Theoretical and Numerical Bases, EPRI, Palo Alto, CA: 2004. 1011307.
21. Fuel Analysis . and Licensing Code: FALCON MOD01: Volume 2: User’s Manual, EPRI, Palo Alto, CA: 2004. 1011308.
22. FALCON MOD01 update 31 with GRSW-A V4.03, Code version manual, Rev.4, 04.11.2020.
23. G. Khvostov. Thermal physical Aspects of Fuel Rod Behavior Modeling Using START-3 Code. IAEA Workshop on Implementation of the WWER version of the TRANSURANUS code and its application to the Safety Criteria, Sofia, Bulgaria, December 7-9, 1998. https://doi.org/10.13140/RG.2.2.30996.91522/1.
24. W. Wiesenack. Assessment of UO2 Conductivity degradation based on In-pile Temperature Data. ITM, Portland, Oregon, March 2-6, 1997.
25. J. Nakamural. Thermal Diffusivity Measurement of High BurnUp UO2 Pellet irradiated at HBWR. Proceedings of OECD/NEA Seminar on the Thermal Performance of High Burnup LWR Fuel, Cadarache, France, March 1998, p. 43.
26. G. Khvostov, V. Novikov, A. Medvedev, S. Bogatyr, “Approaches to Modeling of high burn-up structure and analysis of its effects on the behaviour of light water reactor fuels in the START-3 fuel performance code, Water Reactor Fuel Performance Meeting/WRFPM 2005, 2005. Paper 1104.
27. G. Khvostov, “Analysis of cladding failure in a BWR fuel rod using a SLICE-DO model of the FALCON code”, Nucl. Eng. Technol., vol. 52, no. 12, pp. 2887-2900, 2020. https://doi.org/10.1016/j.net.2020.05.015.
28. H. Assmann, H. Stehle, “Thermal and in-reactor densification of UO2: Mechanisms and experimental results”, Nucl. Eng. Des., vol. 48, pp. 49-67, 2016. https://doi.org/10.1016/0029-5493(78)90208-X.
29. G. Khvostov. Comprehensive Verification of the FALCON (PSI) Code for Calculation of Nuclear Fuel Temperature. Research Proposal, 2019.